Proton Tolerance of Fourth-Generation 350 GHz UHV/CVD SiGe HBTs

Akil K. Sutton, *Student Member, IEEE*, Becca M. Haugerud, *Student Member, IEEE*, Yuan Lu, *Student Member, IEEE*, Wei-Min Lance Kuo, *Student Member, IEEE*, John D. Cressler, *Fellow, IEEE*, Paul W. Marshall, *Member, IEEE*, Robert A. Reed, *Member, IEEE*, Jae-Sung Rieh, *Member, IEEE*, Greg Freeman, *Senior Member, IEEE*, and David Ahlgren

***Abstract*—We report, for the first time, the impact of proton irradiation on fourth-generation SiGe heterojunction bipolar transistors (HBTs) having a record peak unity gain cutoff frequency of 350 GHz. The implications of aggressive vertical scaling on the observed proton tolerance is investigated through comparisons of the pre-and post-radiation ac and dc figures-of-merit to observed results from prior SiGe HBT technology nodes irradiated under identical conditions. In addition, transistors of varying breakdown voltage are used to probe the differences in proton tolerance as a function of collector doping. Our findings indicate that SiGe HBTs continue to exhibit impressive total dose tolerance, even at unprecedented levels of vertical profile scaling and frequency response. Negligible total dose degradation in β (0.3%), f_T and $f_{\max}$(6%) are observed in the circuit bias regime, suggesting that SiGe HBT BiCMOS technology is potentially a formidable contender for high-performance space-borne applications.**

***Index Terms*—Breakdwon voltage, heterojunction bipolar transistors (HBT), proton tolerance, SiGe, silicon-germanium, technology scaling.**

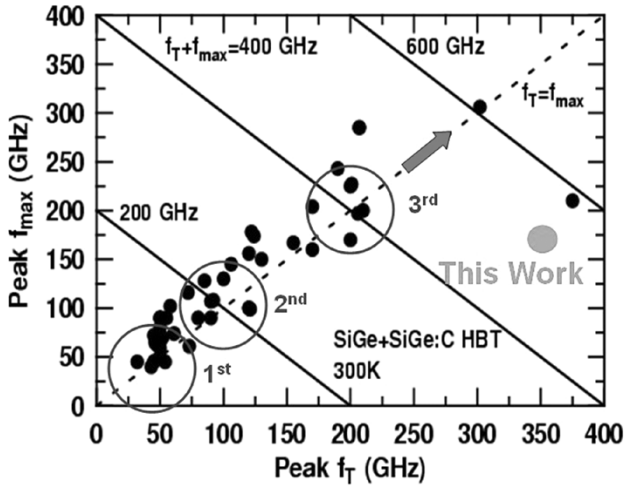

Fig. 1. Comparison of SiGe HBT technology nodes in the f_T-$f_{\max}$ space.

I. Motivation

SILICON–GERMANIUM heterojunction bipolar transistors (SiGe HBTs) continue to emerge as a viable technology option for terrestrial monolithic RF, microwave, and even millimeter IC's used in broadband communications systems. SiGe HBTs exhibit performance characteristics as good as, or better than III-V technologies, while leveraging seamless integration with traditional low cost, high yield Si-based CMOS fabrication [1]. This synergy enables the technology to be incorporated into SiGe BiCMOS system-on-a-chip (SoC) integration schemes that can be tailored to produce "commercial-off-the-shelf" (COTS) modules for communications systems.

The fourth-generation SiGe HBTs under investigation here were fabricated at IBM Microelectronics (IBM 9T), and achieve a remarkable peak cutoff frequency (f_T) of 350 GHz, a record for any Si-based transistor. This unprecedented level of frequency response represents a 67% increase over the previous SiGe HBT performance record, and was fabricated in a 120-nm 100% Si-compatible technology, as detailed in [2]. Process windows currently enable the realization of peak f_T and $f_{\max}$ both above 300 GHz through careful optimization, as recently reported in [3], but the present work features a nonoptimized $f_{\max}$ of 170 GHz, as illustrated in Fig. 1. The associated BV_{CEO} and BV_{CBO} are 1.4 and 5.0 V, respectively, yielding an $f_T BV_{CEO}$ product well above the 200 GHz V "Johnson limit" [4].

The scaling methodologies employed in the first two technology generations (IBM 5HP and 7HP), and the resultant effects on the observed proton tolerance, are described in [5], and are not revisited here. In the third-generation SiGe technology (IBM 8HP), an improvement in f_T, to 200 GHz, was realized primarily through fundamental changes in the physical structure of the transistor. Specifically, a reduced thermal cycle "raised extrinsic base" structure was implemented using conventional deep trench (DT) and shallow trench isolation (STI), in addition to an *in—situ* doped polysilicon emitter. The SiGe base region featured an unconditionally stable, 25% peak Ge, C-doped profile deposited using UHV/CVD epitaxial growth techniques as described in [6].

This new structure, depicted in Fig. 2, raises serious concerns regarding the spatial distribution of radiation induced trap centers previously determined to be primarily located near the STI

Manuscript received July 20, 2004; revised September 6, 2004. This work was supported by DTRA under the Radiation Tolerant Microelectronics Program, NASA-GSFC under the Electronics Radiation Characterization Program, IBM, and the Georgia Electronic Design Center at Georgia Tech.

A. K. Sutton, J. D. Cressler, B. M. Haugerud, W.-M. L. Kuo, and Y. Lu are with the School of Electrical and Computer Engineering, Georgia Institute of Technology, Atlanta, GA 30308 USA (e-mail: asutton@ece.gatech.edu).

P. W. Marshall and R. A. Reed are with a consultant to NASA-GSFC, Greenbelt, MD 20771 USA.

J.-S. Rieh, G. Freeman, and D. Ahlgren are with the IBM Microelectronics, Hopewell Junction, NY 12533 USA.

Digital Object Identifier 10.1109/TNS.2004.839302

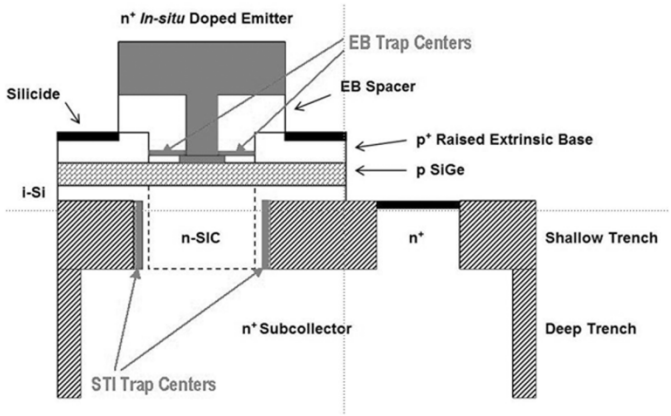

Fig. 2. Representative cross section of a fourth-generation SiGe HBT.

TABLE I
FIRST-, SECOND-, THIRD-, AND FOURTH-GENERATION SIGE HBT FIGURES OF MERIT

Figure of Merit	1^{st}	2^{nd})	3^{rd}	4^{th}
W_E (μm)	0.42	0.18	0.12	0.12
peak f_T (GHz)	50	120	207	300
peak f_{max} (GHz)	70	100	285	170
BV_{CEO} (V)	3.3	2.5	1.7	1.4

edges alongside the emitter-base (EB) spacer [7]. The key performance metrics for the first- through fourth-generation SiGe HBT devices are illustrated in Table I.

Investigations into the proton tolerance of the third-generation structure concluded that these devices were tolerant to total dose effects [8]. It should be noted however, that pre-existing generation-recombination (G/R) trap centers prior to irradiation raise some uncertainty as to the degree of masking of any additional radiation induced traps. In the case of the new fourth-generation technology (same representative cross section as for the third-generation technology), performance enhancements were realized primarily through careful profile optimization and aggressive vertical scaling of the base and collector regions, resulting in a record emitter-to-collector transit time (τ_{EC}) of 0.45 psec [2]. The key fabrication parameters that were adjusted to realize these performance enhancements include the base width (W_b), germanium content, and dopant profiles as highlighted in the representative SIMS doping profile of a first-generation device illustrated in Fig. 3.

The impact of combining this unprecedented level of vertical profile scaling on the proton radiation response is investigated for the first time using these 350 GHz SiGe HBTs. A comprehensive picture of the variation in total dose tolerance across multiple SiGe technology platforms is presented by drawing quantitative comparisons between first (IBM 5HP), second (IBM 7HP), third (IBM 8T), and now fourth (IBM 9T) generation SiGe technology nodes.

II. EXPERIMENT

The fourth-generation 350 GHz SiGe HBTs investigated here feature an emitter area (A_E) of 0.12×2.5 μm^2, and were compared to 0.50 μm 50 GHz (IBM 5HP), 0.20 μm 120 GHz (IBM 7HP), and 0.12 μm 200 GHz (IBM 8T) technology nodes measured under identical conditions in order to facilitate unambiguous comparisons. In the case of the fourth-generation technology, transistors of varying breakdown voltage were used to evaluate the impact of the collector doping profile (peak concentration) on the measured proton response.

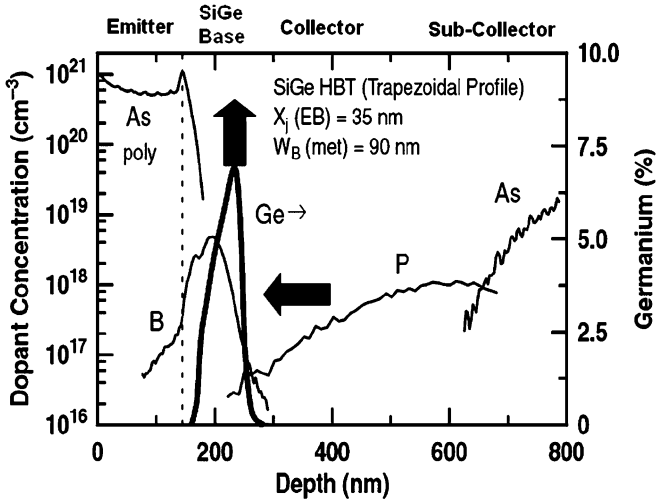

Fig. 3. Representative SIMS profile of a first-generation technology.

The samples were irradiated with 63.3 MeV protons at the Crocker Nuclear Laboratory at the University of California at Davis. The dosimetry measurements used a five-foil secondary emission monitor calibrated against a Faraday cup. The radiation source (Ta scattering foils) located several meters upstream of the target establish a beam spatial uniformity of about 15% over a 2.0 cm radius circular area. Beam currents from about 20 to 100 nA allowed testing with proton fluxes from 1×10^9 to 1×10^{12} proton/cm^{2}s. The dosimetry system has been previously described [9], [10], and is accurate to about 10%. At proton fluences of 1×10^{12} p/cm^2 and 5×10^{13} p/cm^2, the measured equivalent total ionizing dose was approximately 135 and 6,759 krad(Si), respectively. The SiGe HBTs were irradiated with all terminals grounded for the dc measurements and with all terminals floating for the ac measurements at proton fluences ranging from 1.0×10^{12} p/cm^2 to 5.0×10^{13} p/cm^2. Previous investigations have demonstrated that irradiations conducted with all terminals grounded exhibited similar degradation to the case with all terminals floating for first generation devices. These bias conditions are considered "worse case" compared to other bias conditions (Forward active mode, Reverse bias EB junction) [11]. Initial results from proton irradiations of second-generation devices under various bias conditions indicate that all terminals grounded continues to be the worst case. A comprehensive analysis of the bias sensitivty for third- and fourth-generation devices remains to be done.

The ac measurement samples were irradiated at 7.0×10^{12} p/cm^2 and 5.0×10^{13} p/cm^2 with all terminals floating. Wirebonding of ac test structures is not compatible with robust broadband measurements, and hence on-wafer probing of S-parameters (with terminals floating) was used to characterize the high-frequency device performance. The post-irradiated samples were characterized at room temperature with an Agilent 4155 Semiconductor Parameter Analyzer (dc) and an Agilent 8510C Vector Network Analyzer (ac) using the deembedding techniques discussed in [12].

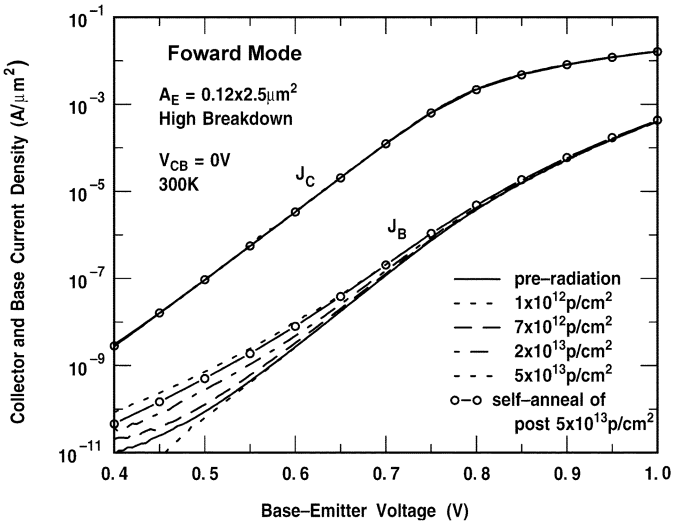

Fig. 4. Forward-mode gummel characteristics (fourth-generation).

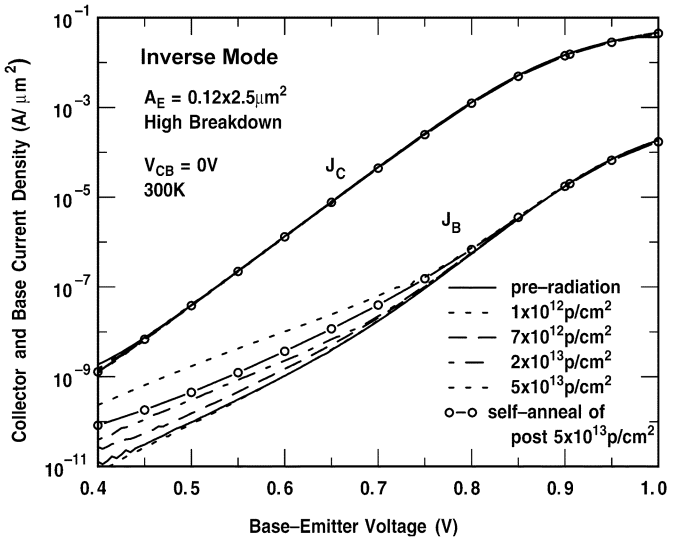

Fig. 5. Inverse-mode gummel characteristics (fourth-generation).

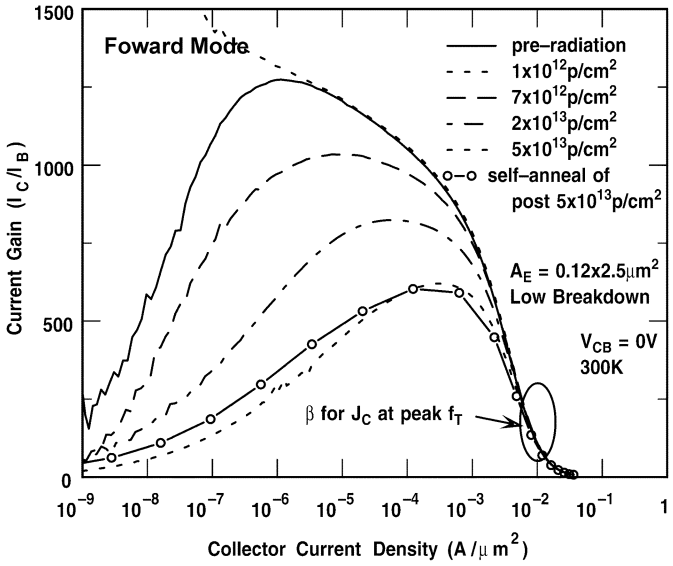

Fig. 6. Forward-mode current gain (fourth-generation).

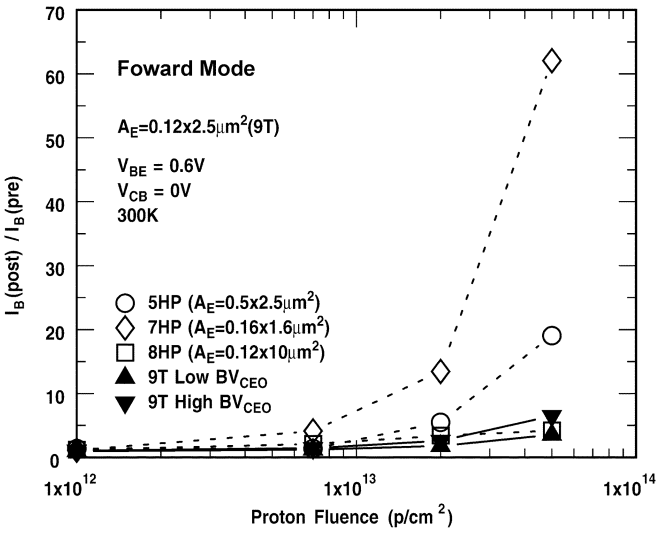

Fig. 7. Forward-mode I_B degradation (first-, second-, third- and fourth-generation).

III. DC Results

The post-irradiation forward-mode Gummel characteristics on a low-breakdown transistor are shown in Fig. 4 and clearly indicate a base current density ($J_B = I_B/A_E$) that is a monotonically increasing function of proton fluence. This classical signature of radiation-induced damage in SiGe HBTs is attributed to radiation-induced G/R trap centers, physically located near the emitter-base spacer oxide and shallow-trench isolation (STI) edges [7]. Measurements performed at room temperature, approximately 6 weeks after the exposure yielded a slight decrease in J_B, indicative of a "self-annealing" mechanism. Similar results obtained for the inverse-mode Gummel characteristics (emitter and collector terminals swapped) are illustrated in Fig. 5. At the low fluence of 1×10^{12} p/cm^2 [135 krad(Si)], there is a slight reduction in both the forward- and inverse-mode J_B at very low base-emitter voltages, presumably the manifestation of an underlying radiation-induced annealing of pre-existing G/R traps.

The forward-mode dc current gain (β) is depicted in Fig. 6, and shows a consistent degradation with increasing proton fluence, as expected. There is over 40% decrease in β_{peak} coincident with a shift in the occurence of β_{peak} to higher J_C. More importantly, however, there is practically no change (less than 0.3% decrease) in β at peak f_T, which is the figure-of-merit of primary concern for most circuit designers.

Three dc figures-of-merit were used to compare the proton tolerance across multiple SiGe HBT technology generations: the β_{peak} degradation, and the forward-mode and inverse-mode I_B degradation (sampled at $V_{BE} = 0.6$ V). The increased radiation-induced I_B leakage in second-generation SiGe HBTs compared to that found in the first- has previously been attributed to the increased electric field in the emitter-base (EB) junction at the device periphery, and is associated with the higher local doping associated with vertical and lateral scaling as demonstrated in [5]. Figs. 7 and 8 depict that there are substantial improvements in both the forward- and inverse-mode post-radiation I_B degradation respectively (for both third-, and fourth-generation). An analysis of β_{peak} degradation, shown in Fig. 9, reveals that the fourth- generation devices, with their improved performance, exhibit a degradation similar to that of the first-

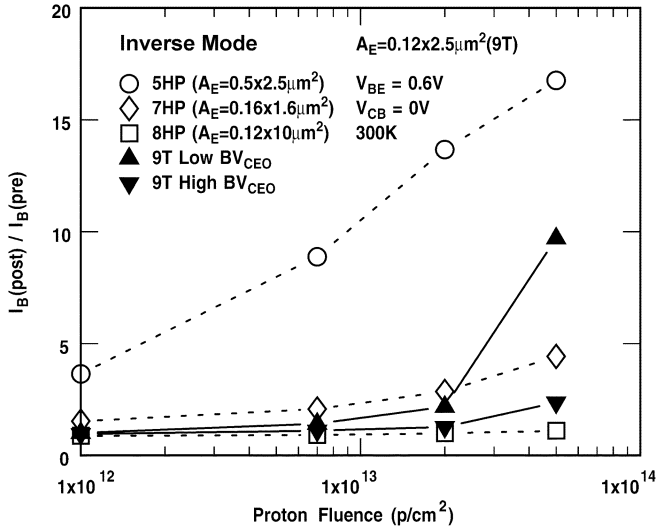

Fig. 8. Inverse-mode I_B degradation (first-, second-, third-, and fourth-generation).

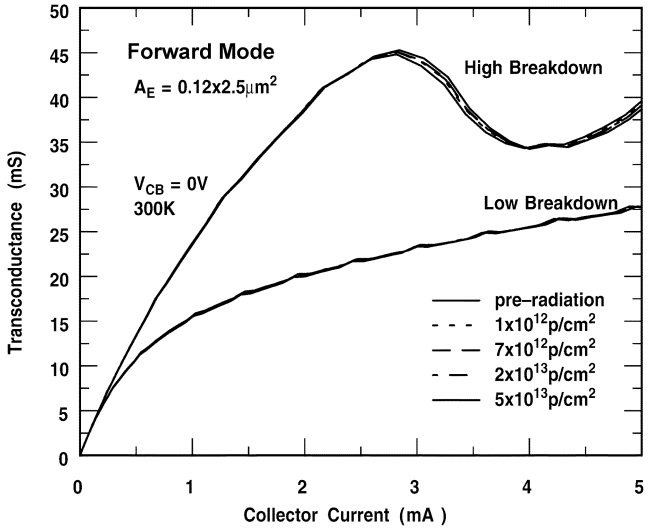

Fig. 10. Extrinsic transconductance for the high- and low-breakdown devices (fourth-generation).

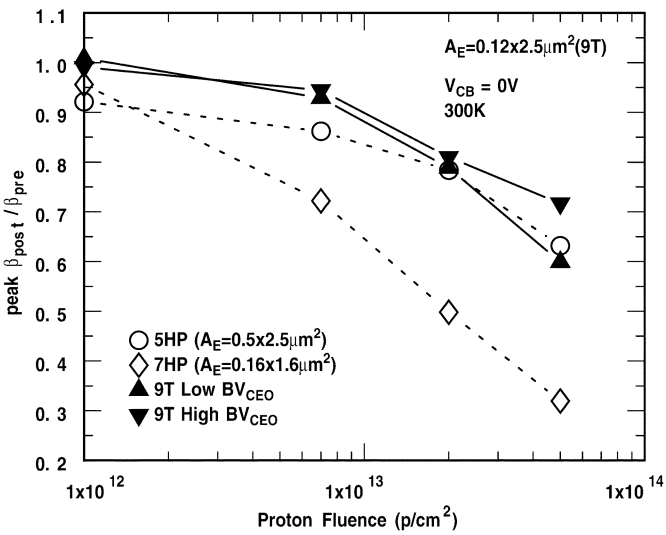

Fig. 9. β_{peak} degradation for for (first-, second-, third-, and fourth-generation).

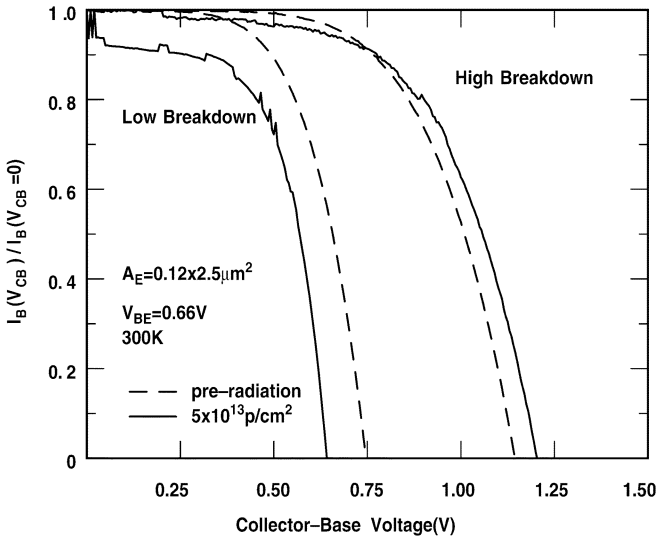

Fig. 11. Neutral base recombination for the high- and low-breakdown devices (fourth-generation).

generation device (and slightly better degradation for the high-breakdown device).

This improved radiation tolerance can be explained by the fact that for both the third-, and fourth- generation devices the "raised extrinsic base" configuration results in EB (*forward—mode*) and CB (*inverse—mode*) junctions that are physically further removed from the STI edges. Therefore, the effective trap density near both of the junctions is such that there is less carrier recombination and hence ΔI_B is reduced. It should be emphasized that these improvements are achieved solely through the migration to the new raised extrinsic base structure and also compare well with the nonideal third- generation devices investigated in [8].

IV. Breakdown Considerations

A closer look at the inverse-mode I_B degradation of the fourth-generation SiGe HBT shown in Fig. 8 indicates that the low-breakdown transistors (with their higher collector doping, N_C) are slightly more susceptible to proton induced damage at the CB junction than those with a higher-breakdown. In the low-breakdown device N_C is increased to delay the onset of high injection heterojunction barrier effects (HBE) and Kirk effect [13]. Typically, this yields an increased collector-base charge capacitance (C_{CB}) and avalanche multiplication $(M-1)$ that results in a reduced $f_{\max}$ and BV_{CEO} respectively [1]. However, careful collector profile optimization can be employed to simultaneously realize improvement in both f_T and BV_{CEO} [14], [15]. In the case of the devices under study, an increased N_C translates into a CB junction now pushed physically closer to the STI edge where the radiation induced G/R trap density is high. The extrinsic transcounductance (g_m) of both high- and low-breakdown devices is shown in Fig. 10. The onset of HBE clearly occurs at a much lower I_C than that of the low-breakdown device, a consequence of the lower N_C doping level in the high-breakdown device and in both cases, is insensitive to proton radiation, clearly good news from a circuit perspective.

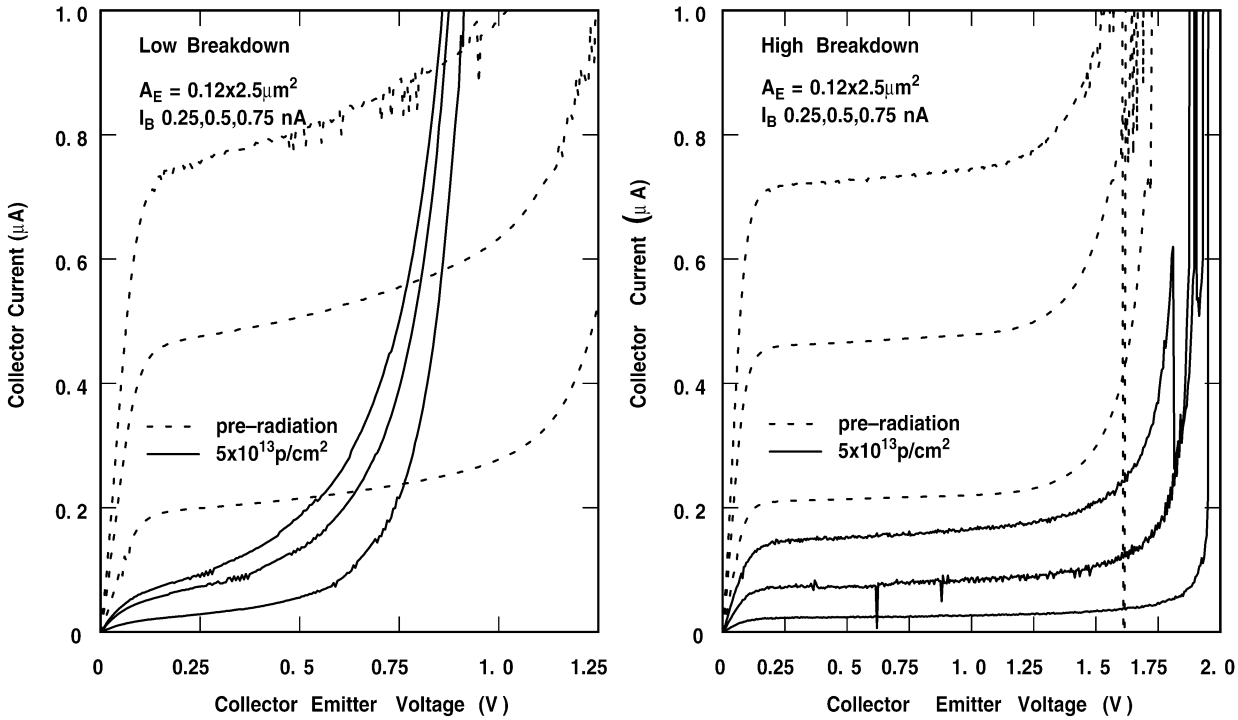

Fig. 12. Forced I_B output characteristics for high- and low-breakdown devices (fourth-generation).

The impact of irradiation on neutral base recombination (NBR) is shown in Fig. 11 for $V_{BE} = 0.66$ V. It is evident that the low-breakdown device, with its increased N_C, exhibits a much stronger post-radiation NBR component at low V_{CB}, as manifested by the increased $I_B(V_{CB})/I_B(0)$ factor. This is the result of increased recombination of minority and majority carriers in the base. Increased base-recombination results in an increase in I_B and reduction in β as observed in Fig. 6. In the case of the high-breakdown device, the post radiation NBR component is significantly less.

Fig. 11 also demonstrates that the breakdown voltage, BV_{CEO} (extracted as the voltage at which $I_B(V_{CB})/I_B(0) = 0$) increases with fluence in the case of the high-breakdown device, but decreases in the case of the low-breakdown device. The low injection, forced-I_B output characteristics depicted in Fig. 12 provide additional evidence of this result. The post-radiation output characterisitics of the low-breakdown device demonstrate increased avalanche multiplication, and a reduced V_A, BV_{CEO}, and β, whereas the results for the high-breakdown device indicate that these effects are not nearly as pronounced, and BV_{CEO} even *increases*. These results indicate again that strong electric fields (as reported in [5]), this time in the CB junction (on account of high N_C), negatively impact the post-radiation device performance characteristics.

V. AC Results

The transistor scattering parameters (S-parameters) for the low-breakdown device ($f_T = 350$ GHz), were characterized to 45 GHz over a range of bias currents, each at a constant V_{CB}. This data was then subsequently de-embedded using standard "open-short" structures to calculate the small-signal current gain ($h_{21} = i_c/i_b\,|_{v_c=0}$) and the Mason's unilateral gain $[U = |Y_{21} - Y_{12}|^2 / 4(G_{11}G_{22} - G_{12}G_{21})]$ described in [16].

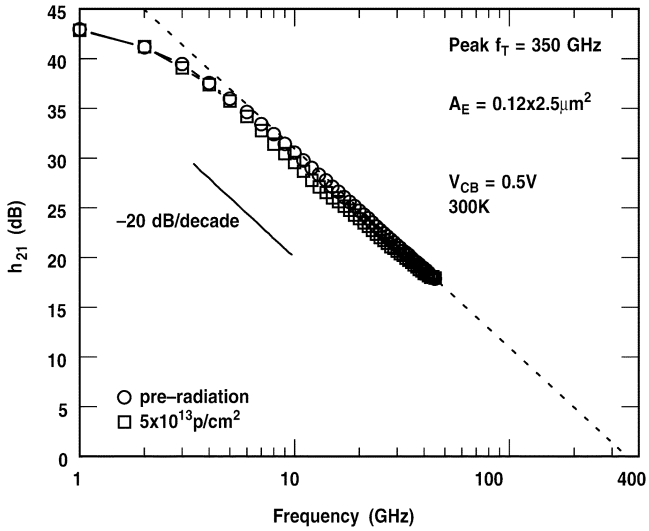

Fig. 13. h_{21} extrapolation for fourth-generation SiGe HBTs.

f_T data points were then obtained using a -20 dB/decade slope extrapolation of h_{21} for different proton fluences, as shown in Fig. 13 for both pre-radiation and a post-radiation fluence of 5×10^{13} p/cm^2. f_T is defined as frequency at which the short circuit current gain of the transistor h_{21}, becomes unity. $f_{\max}$ is determined as the frequency at which the maximum operating power gain $G_{p,\max}$, becomes unity. As evidenced in the figure, both pre- and post-radiation h_{21} data are remarkably robust. An overlay of pre- and post-radiation measurements of f_T vs J_C for first-, second-, third- and fourth-generation SiGe HBTs, shown in Fig. 14 verify that their ac performance continues to be remarkably resistant to proton induced radiation damage by ionizing radiation, even for novel device structures employing both aggressive vertical scaling and reduced thermal

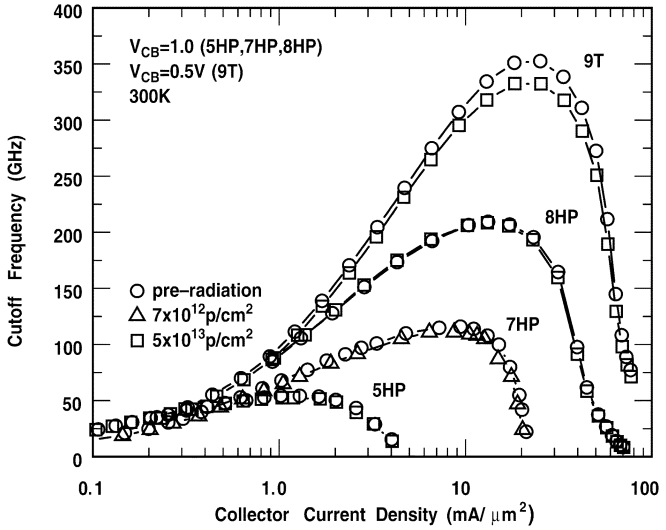

Fig. 14. Pre- and post-radiation f_T for first-, second-, third-, and fourth-generation SiGe HBTs.

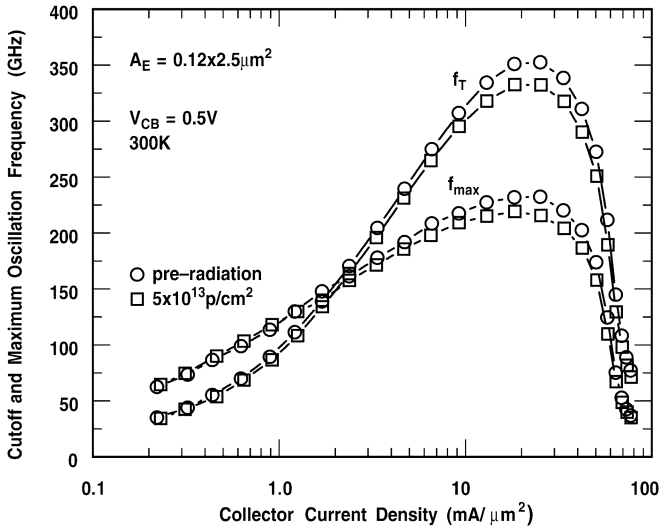

Fig. 15. Pre- and post-radiation f_T and $f_{\max}$ for fourth-generation SiGe HBTs.

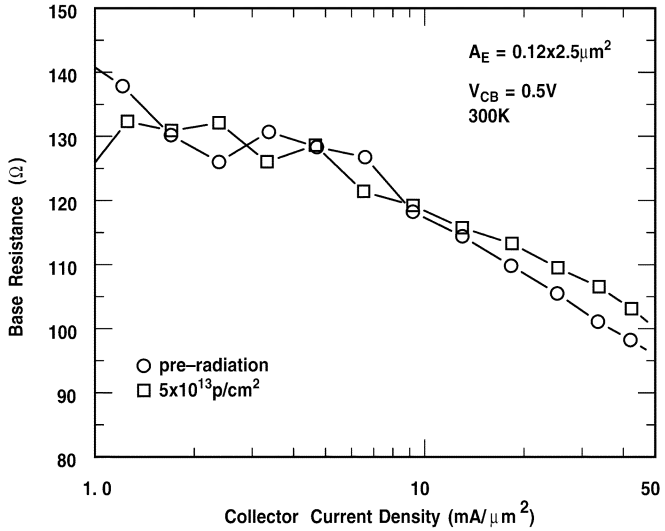

Fig. 16. Pre- and post-radiation r_{bb} variation with J_C (fourth-generation SiGe HBTs).

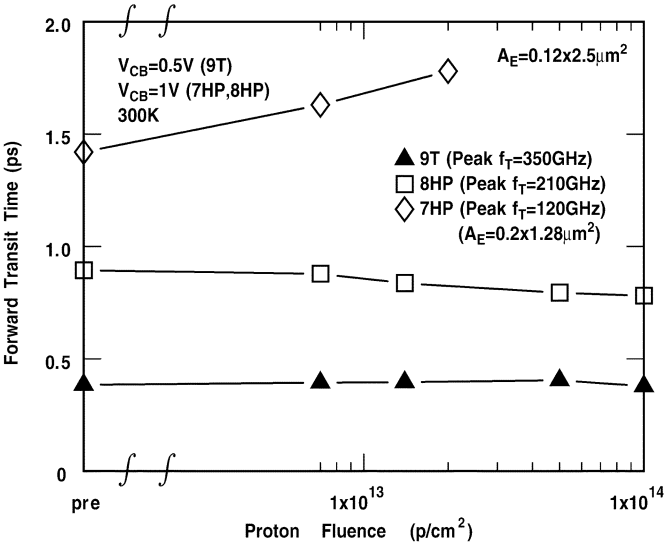

Fig. 17. τ_{EC} variation with fluence for second-, third-, and fourth-generation SiGe HBTs.

cycle processing. This is clearly excellent news. Specifically, in the case of the fourth-generation SiGe HBT there is a moderate 6% decrease in both f_T and $f_{\max}$ as depicted in Fig. 15.

The dynamic base resistance (r_{bb}), was extracted from measured S-parameters and is shown in Fig. 16. A slight increase in r_{bb} at 5×10^{13}p/cm^2, for J_C close to peak f_T is observed and is consistent with the moderate 6% decrease in the peak $f_{\max}$, previously attributed to displacement effects in the neutral base region and the deactivation of boron dopants [8]. For lower J_C values, pre- and post-radiation r_{bb} both exhibit significant fluctuation. This can be attributed to the fact that small-signal parameter extraction in this lower bias regime may be less accurate on account of the smaller dynamic range of the VNA. Finally, the forward transit time (τ_{EC}), as a function of proton fluence, for second-, third- and fourth-generation SiGe HBTs are given in Fig. 17. The vertical scaling methodolgies outlined in [2] enables further reduction in τ_{EC} to a record value of 0.45 ps, as shown in the Figure. More importantly, τ_{EC} remains remarkably independent of proton fluence up to an extreme level of 1×10^{14} p/cm^2 in the case of the third- and fourth-generation SiGe HBT-generation device. This is in stark contrast to the monotonically increasing relationship between τ_{EC} and fluence for the second generation device, an indication that the new raised extrinsic base structure also affords carrier transit paths that are further removed from areas of high radiation induced trap density.

VI. Conclusion

The proton tolerance of fourth-generation SiGe HBTs is assessed through critical analysis of the post-radiation effect on ac and dc figures-of-merit. Specifically a moderate 6% decrease is observed for both f_T and $f_{\max}$ (well within the measurement error of the setup) and β at peak f_T experiences less than 0.3% reduction. Both forward and inverse I_B leakage for the third-

and fourth-generation devices are significantly lower than that of previous technology nodes, a testament to inherent resilience of the raised extrinsic base structure in improving the isolation of the EB and CB junctions from radiation induced traps. Additionally, subtle differences in the response of fourth-generation devices with different collector doping have been explored. These results clearly indicate that SiGe HBTs continue to maintain excellent total dose tolerance in the midst of aggressive technology scaling.

ACKNOWLEDGMENT

The authors would like to thank L. Cohn, K. LaBel, J. Lee, S. Nuttnick, G. Niu, A. Joseph, D. Harame, D. Herman, B. Meyerson, and the IBM SiGe Team for their contributions.

REFERENCES

[1] J. D. Cressler and G. Niu, *Silicon-Germanium Heterojunction Bipolar Transistors*. Boston, MA: Artech House, 2003.

[2] J.-S. Rieh, B. Jagannathan, H. Chen, K. T. Schonenberg, D. Angell, A. Chinthakindi, J. Florkey, F. Golan, D. Greenberg, S.-J. Jeng, M. Khater, F. Pagette, C. Schnabel, P. Smith, A. Stricker, K. Vaed, R. Volant, D. Ahlgren, G. Freeman, K. Stein, and S. Subbanna, "SiGe HBTs with cut-off frequency of 350 GHz," in *IEEE IEDM Tech. Dig.*, 2002, pp. 771–774.

[3] J.-S. Rieh, D. Greenberg, M. Khater, K. T. Schonenberg, S.-J. Jeng, F. Pagette, T. Adam, A. Chinthakindi, J. Florkey, B. Jagannathan, J. Johnson, R. Krishnasamy, D. Sanderson, C. Schnabel, P. Smith, A. Stricker, S. Sweeney, K. Vaed, T. Yanagisawa, D. Ahlgren, K. Stein, and G. Freeman, "SiGe HBTs for millimeter-wave applications with simultaneously optimized f_T and $f_{\max}$ of 300 GHz," in *IEEE RFIC Tech. Dig.*, 2004, pp. 395–398.

[4] E. O. Johnson, "Physical limitations on frequency and power parameters of transistors," *RCA Rev.*, vol. 26, pp. 163–177, 1965.

[5] J. D. Cressler, M. C. Hamilton, G. S. Mullinax, Y. Li, G. Niu, C. J. Marshall, P. W. Marshall, H. S. Kim, M. J. Palmer, A. J. Joseph, and G. Freeman, "The effects of proton irradiation on the lateral and vertical scaling of UHV/CVD SiGe HBT BiCMOS technology," *IEEE Trans. Nucl. Sci.*, vol. 47, pp. 2515–2520, Dec. 2000.

[6] B. Jagannathan, M. Khater, F. Pagette, J.-S. Rieh, D. Angell, H. Chen, J. Florkey, F. Golan, D. R. Greenberg, R. Groves, S. J. Jeng, J. Johnson, E. Mengistu, K. T. Schonenberg, C. M. Schnabel, P. Smith, A. Stricker, D. Ahlgren, G. Freeman, K. Stein, and S. Subbanna, "Self-aligned SiGe NPN transistors with 285 GHz $f_{\max}$ and 207 GHz f_T in a manufacturable technology," *IEEE Electron Device Lett.*, vol. 23, pp. 258–260, May 2002.

[7] J. D. Cressler, R. Krithivasan, G. Zhang, G. Niu, P. W. Marshall, H. S. Kim, R. A. Reed, M. J. Palmer, and A. J. Josephy, "An investigation of the origins of the variable proton tolerance in multiple SiGe HBT BiCMOS technology generations," *IEEE Trans. Nucl. Sci.*, vol. 49, pp. 3203–3207, Dec. 2002.

[8] Y. Lu, J. D. Cressler, R. Krithivasan, Y. Li, R. A. Reed, P. W. Marshall, C. Polar, G. Freeman, and D. Ahlgren, "Proton tolerance of a third generation 0.12 μm 185 GHz SiGe HBT technology," *IEEE Trans. Nuclear Science*, vol. 50, pp. 1811–1815, Dec. 2003.

[9] K. M. Murray, W. J. Stapor, and C. Casteneda, "Calibrated charged particle radiation system with precision dosimetric measurement and control," *Nucl. Instrum. Methods Phys. Res.*, vol. A281, pp. 616–621, Sept. 1989.

[10] P. W. Marshall, C. J. Dale, M. A. Carts, and K. A. Label, "Particle-induced bit erros in high performance fiber optic data links for satellite data management," *IEEE Trans. Nucl. Sci.*, vol. 41, pp. 1958–1965, Dec. 1994.

[11] S. Zhang, J. D. Cressler, G. Niu, C. J. Marshall, P. W. Marshall, H. S. Kim, R. A. Reed, M. J. Palmer, A. J. Joseph, and D. L. Harame, "The effects of operating bias conditions on the proton tolerance of SiGe HBTs," *Solid State Electron.*, vol. 47, pp. 1729–1734, 2003.

[12] S. Zhang, G. Niu, J. D. Cressler, S. D. Clark, and D. C. Ahlgren, "The effects of proton irradiation on the RF performance of SiGe HBTs," *IEEE Trans. Nucl. Sci.*, vol. 46, pp. 1716–1721, Dec. 1999.

[13] C. T. Kirk, "Theory of transistor cutoff frequency falloff at high current densities," *IRE Trans. Electron Devices*, vol. 3, pp. 164–170, 1964.

[14] B. G. Malm, T. Johansson, T. Arnborg, H. Norstrom, J. V. Grahn, and M. Ostling, "Implanted collector profile optimization in a SiGe HBT process," *Solid State Electron.*, vol. 45, pp. 399–404, Mar. 2001.

[15] A. J. Joseph, J. D. Cressler, D. M. Richey, and G. Niu, "Optimization of SiGe HBTs for operation at high current densities," *IEEE Trans. Electron Devices*, vol. 46, pp. 1347–1354, July 1999.

[16] S. J. Mason, "Power gain in feedback amplifiers," *IRE Trans. Circuit Theory*, vol. CT-1, pp. 20–25, 1954.